with B set at regular intervals ($\Delta\theta \sim 10°$) of the rotation angle θ, we obtain a full spatial profile of $|\Phi_{QD}(k_X, k_Y)|^2$. This represents the projection in k space of the probability density of a given electronic state confined in the QD.

The model provides a simple explanation of the magnetic field dependence of the resonant current features e_1 to e_7. In particular, the forbidden nature of the tunneling transition associated with e_4 and e_5 at $B = 0$ T is due to the odd parity of the final state wave function, which corresponds to the first excited state of a QD.

Figure 3A shows the spatial form of $G(B) \sim |\Phi_{QD}(k_X, k_Y)|^2$, in the plane (k_X, k_Y) for the three representative QD states corresponding to the peaks e_2, e_4, and e_7. The measured values of $G(B)$ for two directions of B, parallel and antiparallel to the [01$\bar{1}$] axis, are shown (Fig. 3B). The contour plots reveal the characteristic form of the probability density distribution of a ground state orbital and the characteristic lobes of the higher energy states of the QD. The electron wave function has a biaxial symmetry in the growth plane, with axes corresponding quite closely (within measurement error of 10°) to the main crystallographic directions [01$\bar{1}$] and [$\bar{2}$33]. In particular, detailed examination of the data reveals that the projected probability density of the ground state has an elliptical form, with the major axis along the [01$\bar{1}$] direction.

Although our measurements reveal detailed information about the symmetry of the QD wave functions with respect to the in-plane coordinates, they give us no information about the z dependence. This is directly related to the morphology of the QDs. In general, the dot height is much smaller than the dimensions of the base (*1*). Therefore, the quantization energy of confinement along z is much higher than that for in-plane motion. Our discussion of the magnetotunneling data has made two important and reasonable assumptions. The first is that the motion along z is separable from the in-plane motion. This approximation allows us to label the QD state using the quantum numbers n_1 and n_2 for the in-plane motion and n_3 for motion along z. Our second assumption is that all of the observed peaks involve final (QD) states that share the same type of quantum confinement along z, i.e., have the same value of n_3 (= 0).

In recent years, several different approaches have been used to calculate the eigenstates of QDs. They include perturbation effective mass approaches (*1*), eight-band $k \cdot p$ theory (*10*, *22*, *23*), and empirical pseudopotential models (*24*). Calculations generally depict the form of the wave functions as plots of the probability density in real space, $|\Psi_{QD}(r)|^2$. A tunnel current measurement can provide no information about the phase of the wave function, but, in general, the phase of $\Psi_{QD}(r)$ is easily obtained from a model calculation. Once the phase factor is known, it is a straightforward task for theoreticians to Fourier transform the calculations of the wave function into k space. A direct comparison could then be made with our spatial maps.

Our technique has allowed us to observe successive features in $I(V)$ corresponding to resonant tunneling through a limited number of discrete states whose wave functions display the symmetry of the ground state and first and second excited states of QDs. However, the simple device configuration does not permit us to determine whether an excited state peak and a ground state peak correspond to the same QD. This question could be resolved by experiments on structures with electrostatic gates (*18*).

Despite the large number of QDs in our sample (10^6 to 10^7 for a 100-μm-diameter mesa), we observed only a small number of resonant peaks over the bias range (~100 mV) close to the threshold for current flow. This behavior has been reported in earlier studies (*13*–*18*) and, although not fully understood, is probably related to the limited number of conducting channels in the emitter that can transmit electrons from the doping layer to the QDs at low bias. There is no reason to believe that the dots studied are atypical of the distribution as a whole.

Magnetotunneling spectroscopy provides us with a means of probing the spatial form of the wave functions of electrons confined in zero-dimensional QDs. The technique is both noninvasive and nondestructive and allows us to probe spatially quantum states that are buried hundreds of nanometers below the surface.

References and Notes

1. D. Bimberg, M. Grundmann, N. N. Ledentsov, *Quantum Dot Heterostructures* (Wiley, New York, 1999), and references therein.
2. J. Y. Marzin, J. M. Gerard, A. Izraël, D. Barrier, G. Bastard, *Phys. Rev. Lett.* **73**, 716 (1994).
3. R. J. Nötzel, J. Temmyo, T. Tamamura, *Nature* **369**, 131 (1994).
4. L. Landin, M. S. Miller, M.-E. Pistol, C. E. Pryor, L. Samuelson, *Science* **280**, 262 (1998).
5. A. P. Alivisatos, *Science* **271**, 933 (1996).
6. S. A. Empedocles and M. G. Bawendi, *Science* **278**, 2114 (1997).
7. M. F. Crommie, C. P. Lutz, D. M. Eigler, *Science* **262**, 218 (1993).
8. S. H. Pan *et al.*, *Nature* **403**, 746 (2000).
9. N. B. Zhitenev *et al.*, *Nature* **404**, 473 (2000).
10. O. Stier, M. Grundmann, D. Bimberg, *Phys. Rev. B* **59**, 5688 (1999).
11. A. Patanè *et al.*, *Phys. Rev. B*, in press.
12. A. K. Geim *et al.*, *Phys. Rev. Lett.* **72**, 2061 (1994).
13. P. C. Main *et al.*, *Phys. Rev. Lett.* **84**, 729 (2000).
14. M. Narihiro, G. Yusa, Y. Nakamura, T. Noda, H. Sakaki, *Appl. Phys. Lett.* **70**, 105 (1997).
15. I. E. Itskevich *et al.*, *Phys. Rev. B* **54**, 16401 (1996).
16. I. Hapke-Wurst *et al.*, *Semicond. Sci. Technol.* **14**, L41 (1999).
17. T. Suzuki, K. Nomoto, K. Taira, I. Hase, *Jpn. J. Appl. Phys. Part 1* **36**, 1917 (1997).
18. D. G. Austing *et al.*, *Appl. Phys. Lett.* **75**, 671 (1999).
19. R. K. Hayden *et al.*, *Phys. Rev. Lett.* **66**, 1749 (1991).
20. P. H. Beton *et al.*, *Phys. Rev. Lett.* **75**, 1996 (1995).
21. J. W. Sakai *et al.*, *Phys. Rev. B* **48**, 5664 (1993).
22. C. Pryor, *Phys. Rev. B* **57**, 7190 (1998).
23. W. Yang, H. Lee, T. J. Jonhson, P. C. Sercel, A. G. Norman, *Phys. Rev. B* **61**, 2784 (2000).
24. L.-W. Wang, J. Kim, A. Zunger, *Phys. Rev. B* **59**, 5678 (1999).

25. The work is supported by the Engineering and Physical Sciences Research Council (UK). A.L. gratefully acknowledges the support of the Fundação de Ampàro Pesquia do Estado de São Paulo Foundation (Brazil). E.E.V. and Y.V.D. gratefully acknowledge support from the Royal Society.

21 June 2000; accepted 16 August 2000

Potent Analgesic Effects of GDNF in Neuropathic Pain States

Timothy J. Boucher,[1] Kenji Okuse,[2] David L. H. Bennett,[1]* John B. Munson,[1] John N. Wood,[2] Stephen B. McMahon[1]†

Neuropathic pain arises as a debilitating consequence of nerve injury. The etiology of such pain is poorly understood, and existing treatment is largely ineffective. We demonstrate here that glial cell line–derived neurotrophic factor (GDNF) both prevented and reversed sensory abnormalities that developed in neuropathic pain models, without affecting pain-related behavior in normal animals. GDNF reduces ectopic discharges within sensory neurons after nerve injury. This may arise as a consequence of the reversal by GDNF of the injury-induced plasticity of several sodium channel subunits. Together these findings provide a rational basis for the use of GDNF as a therapeutic treatment for neuropathic pain states.

The neurotrophic factor GDNF promotes survival of a subgroup of developing sensory neurons (*1*). In adult animals, approximately 60% of dorsal root ganglion neurons normally express receptor components for GDNF (*2*, *3*), and this factor promotes neurite outgrowth in vitro and regeneration in vivo of both large- and small-caliber sensory neurons (*4*, *5*). GDNF is known to have neuroprotective effects on damaged adult sensory neurons, including the reversal of axotomy-induced changes in gene expression (*2*, *6*, *7*).

One of the most important functional consequences of peripheral nerve damage is the emergence of neuropathic pain. Such pains are often intense, persistent, and refractory to existing analgesic therapy. Here, we have examined the ability of GDNF to reverse the sensory abnormalities found in animal models of neuropathic pain and have studied putative mechanisms of action.

Adult rats received a partial ligation of one sciatic nerve (*8*) and continuous concurrent intrathecal infusion of GDNF or vehicle (*9*). Ipsilateral paw sensitivity to mechanical and thermal stimuli was assessed. Vehicle-treated animals developed significant mechanical and thermal hyperalgesia (drop of flexion-withdrawal thresholds from 12.1 ± 1 to 2.2 ± 0.3 g, noxious heat-induced paw withdrawal latency from 11.9 ± 0.5 to 7.4 ± 0.5 s, $P < 0.01$; Fig. 1A). These changes were seen within 2 days, persisting throughout the 15-day observation period (*8*). With GDNF treatment, neither mechanical nor thermal hyperalgesia developed (no change in threshold from baseline values at any time after surgery, $P > 0.1$; Fig. 1A). In a second model, animals received a fifth lumbar (L5) spinal nerve ligation [modified from (*10*)] with intrathecal GDNF or vehicle as before (*9*). Vehicle-treated animals developed profound hyperalgesia ($P < 0.01$); infusion of GDNF prevented any significant changes from preoperative baselines (Fig. 1B). Identical treatment with biologically active doses of nerve growth factor (NGF) or the neurotrophin NT-3 (*5*, *11*) had no effect on the emergence or degree of sensory abnormality (Fig. 1B).

We then started GDNF treatment 2 days after spinal nerve ligation. Mechanical and thermal hyperalgesia developed within 2 days (drop from 12.7 ± 1.5 to 3 ± 0.6 g, 11.4 ± 0.3 to 9.1 ± 0.5 s, $P < 0.01$; Fig. 1C). These persisted in vehicle-treated animals ($P < 0.01$) but were reversed by GDNF treatment, after which thresholds reverted to normal levels ($P > 0.1$). Hyperalgesia reemerged within 3 days of cessation of GDNF infusion ($P < 0.01$). Identical chronic administration of GDNF to normal animals led to no change in responses to noxious thermal or mechanical stimuli; withdrawal thresholds did not significantly vary from baseline values (13 ± 1 g, 13 ± 0.5 s; $P > 0.1$). Acute peripheral treatment with GDNF (plantar injections of 0.1, 1, and 10 μg) did not affect pain-related behavior; thermal withdrawal thresholds did not significantly differ from baseline values when tested 0, 2, 4, 6, and 24 hours after injection ($P > 0.5$).

A critical and necessary event for neuropathic pain is the development of spontaneous activity following nerve damage (*12*). This activity arises from damaged neurons themselves and from those whose axons are intact but comingle in peripheral nerves along with degenerating axons [(*13*), see (*14*)]. Therefore, we studied ectopic activity in both L5 and L4 DRG neurons after spinal nerve ligation of L5 alone and tested the effects of GDNF treatment (*15*). In the L5 dorsal root 3 and 7 days after this injury, 31 ± 3 and 19 ± 2% of damaged myelinated sensory fibers exhibited spontaneous activity, compared with essentially zero in the acutely cut nerve (1237 myelinated units sampled; Fig. 2A). Mean spontaneous activity was 23 ± 2 spikes per second. No spontaneous activity was seen in C fibers at these time points (0/197 units). With GDNF treatment, fewer fibers exhibited spontaneous discharges (18 ± 1 and 11 ± 1% at 3 and 7 days, respectively; $P < 0.01$, ANOVA), and these units discharged less frequently (14 ± 2 spikes per second; $P < 0.05$, t test). Thus, the afferent barrage entering the cord was greatly reduced (from 6.7 ± 0.7 to 2.5 ± 0.4 impulses per second per myelinated fiber; $P < 0.01$, t test; Fig. 2B). Using spike-triggered averaging, we found that spontaneously active units were among the slower conducting A fibers (Fig. 3B). GDNF selectively prevented ectopic activity in the slowest of these ($P < 0.05$, Kolmogorov-Smirnov test).

Qualitatively similar changes were seen in the L4 dorsal root after L5 spinal nerve ligation, with 14 ± 2% of myelinated sensory fibers exhibiting spontaneous activity (270 units sampled), averaging 16 ± 2 spikes per second. With GDNF treatment, fewer L4 fibers exhibited ectopic discharges (3 ± 2%; $P < 0.01$, t test), and the afferent barrage was reduced from 2.5 ± 0.5 to 0.7 ± 0.5 impulses per second per myelinated fiber ($P < 0.03$, t test; Fig. 2B). The conduction velocity of spontaneously active units in L4 was not significantly different from that of silent units, suggesting that most were low-threshold mechanoreceptors ($P > 0.1$, t test; Fig.

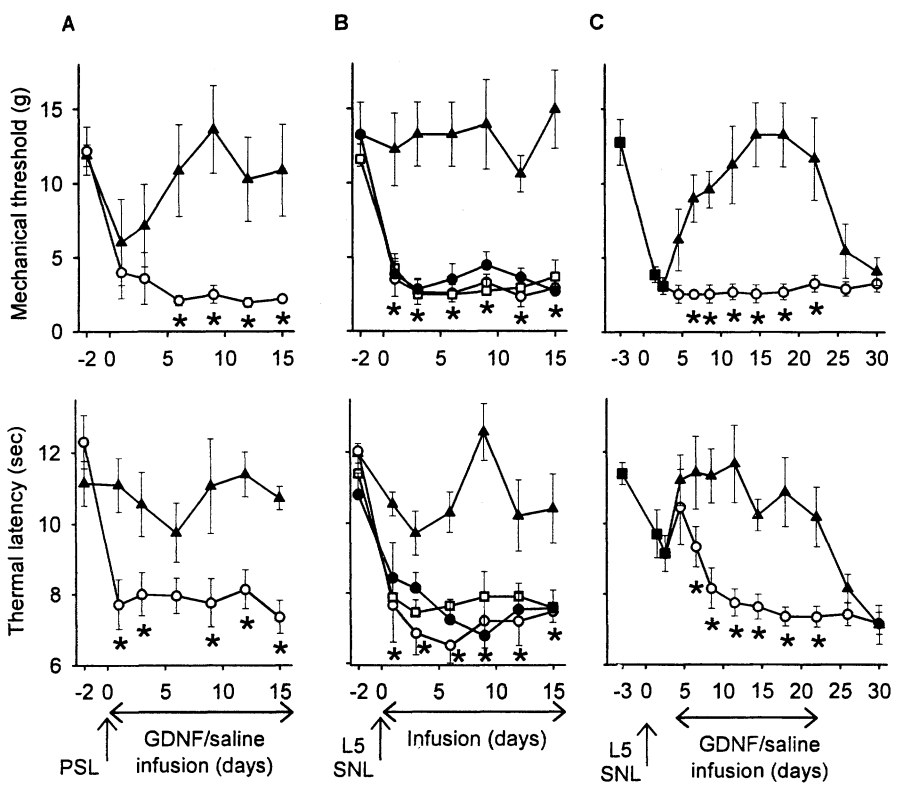

Fig. 1. Nociceptive responses of animals subjected to either partial sciatic ligation (PSL) or L5 spinal nerve ligation (SNL) combined with trophic factor treatment. Mechanical (upper) and thermal (lower) thresholds were tested. (**A**) PSL results in mechanical and thermal hyperalgesia in vehicle-treated animals (open circles). GDNF prevented the development of these sensory abnormalities (filled triangles). (**B**) L5 SNL also results in mechanical and thermal hyperalgesia. Intrathecal GDNF, but not NGF (open squares), NT-3 (filled circles), or vehicle prevented this. (**C**) Delayed infusion of GDNF but not saline reverses the sensory abnormalities established by a previous L5 SNL. The cessation of GDNF infusion results in the reemergence of hyperalgesia. Asterisks denote significant difference between vehicle- and GDNF-treated animals on each testing day (mean ± SEM; see text for details). Filled squares denote pretreatment thresholds.

[1]Centre for Neuroscience Research, King's College London, London SE1 7EH, UK. [2]Department of Biology, University College London, London, WC1E 6BT UK.

*Present address: Department of Medicine, University College Hospital, London WC1E 6AU, UK.

†To whom correspondence should be addressed. E-mail: stephen.mcmahon@kcl.ac.uk

3A). GDNF prevented ectopic activity across this range of conduction velocities (distribution of saline and GDNF-treated units not significantly different, $P > 0.05$, Kolmogorov-Smirnov). No spontaneous activity was seen in C fibers in L4.

Ectopic activity in damaged nerves can be blocked with low concentrations of tetrodotoxin (TTX), suggesting a role for TTX-sensitive sodium channels in this event (*16*). Nerve damage induces novel, rapidly reprimming sodium-channel activity (*17*). Concomitantly, transcripts encoding the type III embryonic sodium channel are up-regulated, and the two TTX-resistant channels in DRG neurons, SNS and NaN, are down-regulated (*18*). We examined the transcript levels of SNS, NaN, and the type III channel in the L4 and L5 DRG after L5 spinal nerve ligation using reverse transcriptase–polymerase chain reaction (RT-PCR) (*19*). In L5, expression of the type III channel was increased, and SNS and NaN transcripts were decreased after this injury (Fig. 4A). By using PCR conditions in the linear range (*19*), densitometric analysis of band intensity showed an increase in type III expression (26 ± 6 to 180 ± 21, arbitrary units) and decreases in SNS and NaN expression (146 ± 12 to 58 ± 8 and 180 ± 8 to 100 ± 23 respectively; $P < 0.05$, ANOVA; Fig. 4B). The only significant change in the L4 DRG 7 days after L5 spinal nerve ligation was an increase in SNS expression (185 ± 5 to 307 ± 2, arbitrary units; $P < 0.001$, ANOVA). GDNF treatment suppressed expression of the type III channel and partially restored SNS and NaN levels in L5 (mean band intensities 54 ± 12, 117 ± 12, 137 ± 33 respectively; not significantly different from naïve, $P > 0.1$, ANOVA), but had no effect on the subunits measured in L4. Changes in TTX-resistant channels are therefore poorly correlated with ectopic activity and neuropathic pain behavior. Plasticity of type III expression in damaged afferents is consistent with a significant role for it in the pathogenesis of neuropathic pain (*20*). The lack of significant changes in L4 may reflect the lower incidence

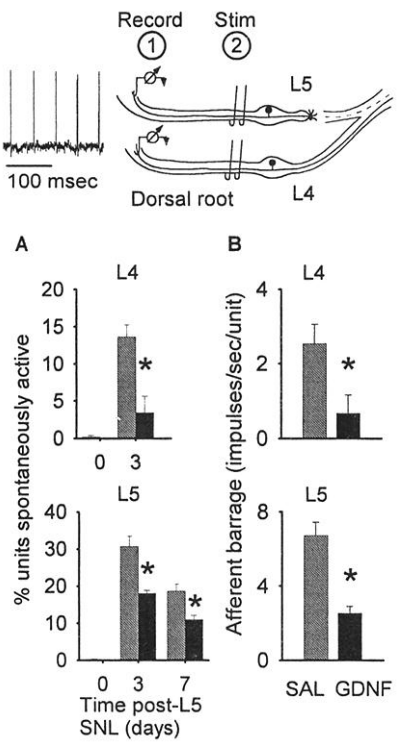

Fig. 2. GDNF reduces ectopic discharges in L4 and L5 sensory neurons following L5 spinal nerve ligation. (**Top**) Spontaneously active units were recorded from fine strands of the L4 or L5 dorsal root (circled 1) (example inset), and the total number of units in each strand was calculated by stimulating the whole root (circled 2). For L4 recordings the L4 spinal nerve was acutely cut 10 mm distal to the DRG. (**A**) L5 spinal nerve ligation induces spontaneous activity in many L4 and L5 myelinated afferents. This effect is markedly reduced by intrathecal GDNF treatment. (**B**) GDNF reduces the proportion and firing frequency of ectopically discharging units, thereby dramatically decreasing the total afferent barrage entering the spinal cord. Asterisks denote significant difference between vehicle- and GDNF-treated animals (mean ± SEM; see text for details).

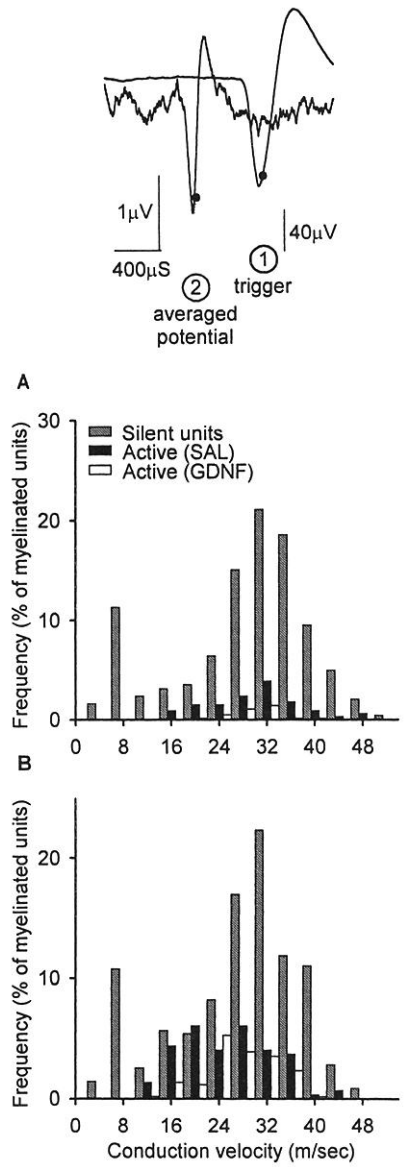

Fig. 3. The conduction velocity of spontaneously active sensory neurons after L5 spinal nerve ligation was estimated by spike-triggered averaging. (**Top**) A spontaneously active unit in the dorsal root (circled 1) triggered a retrospective averaged recording in the appropriate whole root (circled 2). The conduction velocity of silent afferents was calculated from the stimulation experiments shown in Fig. 2. For L4 sensory neurons (**A**), ectopic firing is seen in units with a wide range of conduction velocities, and the whole of this range appears to be affected by GDNF treatment. For L5 sensory neurons (**B**), spontaneously active units are a slower subset of myelinated fibers, and GDNF treatment selectively affects the slowest of these. These slower conducting afferents may have been erstwhile myelinated nociceptors, or fibers representative of the whole population of myelinated afferents but particularly slowed following axotomy.

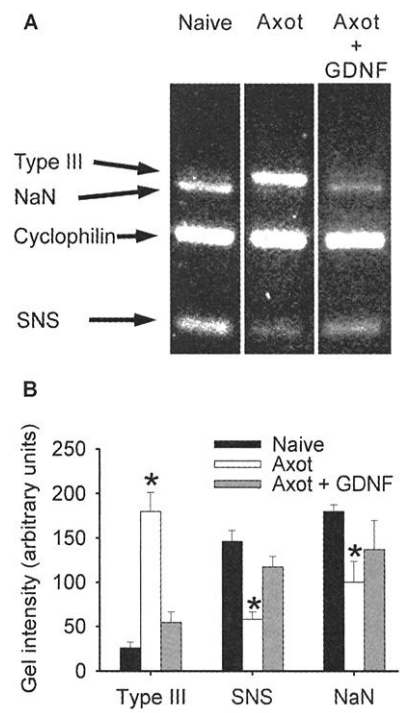

Fig. 4. Altered expression of sensory neuron sodium channel α subunits after L5 spinal nerve ligation: effects of GDNF treatment. RT-PCR analysis of L5 DRG RNA extracts from naïve and nerve-injured rats treated with GDNF or vehicle. RT-PCR reactions using primer pairs for type III, NaN, cyclophilin, and SNS were added to the reaction mixture (*19*). (**A**) Nerve injury up-regulates type III and down-regulates NaN and SNS; treatment with GDNF prevents the novel expression of the type III channel and partially restores SNS and NaN transcripts. (**B**) Densitometric analysis of band intensity across each experimental group. Asterisks denote significant difference from naïve; $P < 0.05$, ANOVA.

of ectopic activity in these neurons and/or other contributory mechanisms.

The nerve damage that precipitates neuropathic pain leads to many changes in sensory neurons, including alterations in putative neurotransmitters/modulators, receptors, ion channels, structural proteins, and anatomic terminations (*21*). The relative contributions of these reactive changes are currently unknown, especially the role of small-caliber nociceptive neurons or large-caliber mechanosensitive afferents (*22*). There is conflicting evidence regarding the role of nociceptors. Antisense treatment against SNS (normally expressed in nociceptors) reduces neuropathic pain behavior (*23*). However, few unmyelinated afferents discharge ectopically in neuropathic models (*24*), and mechanical hyperalgesia is unaffected by the C fiber toxin RTX (*25*). We have also found that the development of neuropathic pain behavior is unaffected in null mutant mice lacking the SNS channel (*26*). In contrast, the data here and in the literature support a pivotal role for myelinated afferents in the generation of neuropathic pain: animal models show that an essential drive for abnormal pain sensitivity is the generation of ectopic activity in damaged sensory neurons (*12*, *27*), arising almost exclusively in myelinated neurons; in human neuropathic pain states, activation of large Aβ afferents is capable of inducing pain (*28*); selective lesions of large myelinated afferents reduce neuropathic pain behavior in animals (*29*).

The ectopic activity that arises in neuropathic conditions is TTX-sensitive. Only the expression of the TTX-sensitive type III α subunit is known to increase following nerve injury (*20*), and we show here that GDNF prevents this. It is unclear whether GDNF acts tonically to repress type III expression under normal circumstances. As GDNF treatment does not affect pain-related behavior in normal animals, the analgesic actions reported here are unlikely to represent general effects on pain signaling systems. However, as GDNF regulates the expression of a variety of genes in both large- and small-caliber sensory neurons, including some functionally relevant for nociceptive behavior [P2X3 and VR1 (*6*, *7*)], effects other than those on the type III sodium channel may contribute to its analgesic actions. This question can only be definitively addressed with specific, type III channel blockers, which have yet to be developed. However, the data presented here provide a rational basis for, and demonstrate the efficacy of, GDNF in the treatment of neuropathic pain.

References and Notes

1. A. Buj-Bello, V. L. Buchman, A. Horton, A. Rosenthal, A. M. Davies, *Neuron* **15**, 821 (1995).
2. D. L. H. Bennett *et al.*, *J. Neurosci.* **18**, 3059 (1998).
3. D. C. Molliver *et al.*, *Neuron* **19**, 849 (1997).
4. P. Leclere *et al.*, *Neuroscience* **82**, 545 (1998).
5. M. S. Ramer, J. V. Priestley, S. B. McMahon, *Nature* **403**, 312 (2000).
6. E. J. Bradbury, G. Burnstock, S. B. McMahon, *Mol. Cell. Neurosci.* **12**, 256 (1998).
7. P. Ogun-Muyiwa, R. Helliwell, P. McIntyre, J. Winter, *Neuroreport* **10**, 2107 (1999).
8. Z. Seltzer, R. Dubner, Y. Shir, *Pain* **43**, 205 (1990).
9. Experiments were carried out in accordance with the UK Animals (Scientific Procedures) Act 1986. Trophic factors were delivered at 12 μg/day (*2*). See (*30*) for details of surgery as well as behavioral and statistical analyses.
10. S. H. Kim and J. M. Chung, *Pain* **50**, 355 (1992).
11. E. J. Bradbury, S. Khemani, V. R. King, J. V. Priestley, S. B. McMahon, *Eur. J. Neurosci.* **11**, 3873 (1999).
12. K. Sheen and J. M. Chung, *Brain Res.* **610**, 62 (1993).
13. M. Michaelis, X. Liu, W. Janig, *J. Neurosci.* **20**, 2742 (2000)
14. Y. Li, M. J. Dorsi, R. A. Meyer, A. J. Belzberg, *Pain* **85**, 493 (2000).
15. See (*30*) for details of recording ectopic discharges in primary afferent neurons.
16. I. Omana-Zapata, M. A. Khabbaz, J. C. Hunter, D. E. Clarke, K. R. Bley, *Pain* **72**, 41 (1997).
17. J. A. Black *et al.*, *J. Neurophysiol.* **82**, 2776 (1999).
18. J. Fjell *et al.*, *Brain Res. Mol. Brain Res.* **67**, 267 (1999).
19. See (*30*) for details of RT-PCR analysis of sodium channel expression in sensory neurons.
20. S. G. Waxman, *Pain* **S6**, S133 (1999).
21. T. J. Boucher, B. J. Kerr, M. S. Ramer, S. W. N. Thompson, S. B. McMahon, *Proc. 9th World Congr. Pain* **16**, 175 (2000).
22. M. S. Gold, *Pain* **84**, 117 (2000).
23. J. Lai, J. C. Hunter, M. H. Ossipov, F. Porreca, *Methods Enzymol.* **314**, 201 (2000).
24. X. Liu, S. Eschenfelder, K.-H. Blenk, W. Jänig, H.-J. Häbler, *Pain* **84**, 309 (2000).
25. M. H. Ossipov, D. Bian, T. P. J. Malan, J. Lai, F. Porreca, *Pain* **79**, 127 (1999).
26. B. J. Kerr, S. B. McMahon, J. N. Wood, unpublished observations.
27. Y. W. Yoon, H. S. Na, J. M. Chung, *Pain* **64**, 27 (1996).
28. J. N. Campbell, S. N. Raja, R. A. Meyer, S. B. Mackinnon, *Pain* **32**, 89 (1988).
29. D. Bian, M. H. Ossipov, C. Zhong, T. P. Malan, F. Porreca, *Neurosci. Lett.* **241**, (1998).
30. Supplementary material is available at www.sciencemag.org/feature/data/1054233.shl.

31. We thank V. Cheah for expert technical assistance, Amgen for supplying rhGDNF, and Genentech for the gift of rhNGF and rhNT-3. This work was supported by the Medical Research Council (T.J.B., D.L.H.B., J.B.M., J.N.W., and S.B.M.) and the Wellcome Trust (J.N.W., K.O., and S.B.M.).

21 July 2000; accepted 22 August 2000

Long-Term Survival But Impaired Homeostatic Proliferation of Naïve T Cells in the Absence of p56^{lck}

Benedict Seddon,[1] Giuseppe Legname,[2] Peter Tomlinson,[1] Rose Zamoyska[1]*

Interactions between the T cell receptor (TCR) and major histocompatibility complex antigens are essential for the survival and homeostasis of peripheral T lymphocytes. However, little is known about the TCR signaling events that result from these interactions. The peripheral T cell pool of p56^{lck} (lck)–deficient mice was reconstituted by the expression of an inducible lck transgene. Continued survival of peripheral naïve T cells was observed for long periods after switching off the transgene. Adoptive transfer of T cells from these mice into T lymphopoienic hosts confirmed that T cell survival was independent of lck but revealed its essential role in TCR-driven homeostatic proliferation of naïve T cells in response to the T cell–deficient host environment. These data suggest that survival and homeostatic expansion depend on different signals.

Despite environmental antigenic stimulation and thymic production, the size of the peripheral T cell pool is maintained at a remarkably constant level (*1*). In common with cells of other tissues, T cells require specific signals in order to survive. In contrast to memory T cells (*2–4*), naïve T cells require interactions of the TCR with self major histocompatibility complex (MHC) antigens for their prolonged survival (*5–10*). Furthermore, T cells also have the capacity to proliferate under T lymphopoienic conditions, and for naïve T cells this too requires recognition of self MHC antigens (*8*, *11–13*). However, less is known about the TCR signals that govern these processes. The src family protein tyrosine kinase p56^{lck} (lck) is involved in the most proximal phosphorylation events during TCR signaling and plays crucial roles at multiple points in T cell development (*14*, *15*). It seemed likely, therefore, that lck would play a critical role in the transduction of survival and homeostatic signals through the TCR.

To evaluate the role of lck in T cell homeostasis, we produced mice that express lck in

[1]Division of Molecular Immunology, National Institute for Medical Research, The Ridgeway, Mill Hill, London NW7 1AA, UK. [2]Institute for Neurodegenerative Diseases, University of California–San Francisco, San Francisco, CA 94143, USA.

*To whom correspondence should be addressed. E-mail: rzamoys@nimr.mrc.ac.uk